Reversible CO_2 Capture and On-Demand Release by an Acidity-Matched Organic Photoswitch

Abdulrahman M. Alfaraidi,[a] Bryan Kudisch,[a] Nina Ni,[a] Jayden Thomas,[a] Thomas Y. George,[b] Khashayar Rajabimoghadam,[a] Haihui Joy Jiang,[a] Daniel G. Nocera,[a] Michael J. Aziz,[b] Richard Y. Liu[a,*]

[a]Department of Chemistry and Chemical Biology, Harvard University, Cambridge, MA 02138, USA

[b]Harvard John A. Paulson School of Engineering and Applied Sciences, Cambridge, MA 02138, USA

[*]E-mail: richardliu@chemistry.harvard.edu

ABSTRACT

Separation of carbon dioxide (CO_2) from point sources or directly from the atmosphere can contribute crucially to climate-change mitigation plans for the coming decades. A fundamental practical limitation for current strategies is the considerable energy cost required to regenerate the sorbent and release the captured CO_2 for storage or utilization. The feasibility of these approaches, including thermal stripping, pressure swing desorption, and electrochemical switching, can only be justified by the availability of affordable, storable, and widely distributable renewable energy. A photochemically driven system that demonstrates efficient passive capture and on-demand CO_2 release triggered by sunlight as the sole external stimulus would provide an attractive alternative. However, little is known about the thermodynamic requirements for such a process, nor mechanisms for modulating changes in CO_2 affinity with photoinduced metastable states. Here, we show that an organic photoswitchable molecule of precisely matched effective acidity can repeatedly capture and release a near-stoichiometric quantity of CO_2 according to dark–light cycles. We show that the CO_2-derived species rests as a solvent-separated ion pair, and key aspects of its excited-state dynamics that regulate photorelease efficiency are characterized by transient absorption spectroscopy. The thermodynamic and kinetic concepts established herein will serve as guiding principles for the development of viable solar-powered negative emissions technologies.

The accumulation of CO_2 in the atmosphere is a primary driver of anthropogenic climate change, and a dramatic reduction of net emissions is urgently required to avoid catastrophic future scenarios.[1,2,3,4] Accordingly, considerable research effort has been dedicated to chemical systems for removing CO_2 from emission streams (CCS, carbon capture and storage)[5,6] and, more recently, from the atmosphere (DAC, direct air capture).[7,8] The most developed technologies for CO_2 capture depend on sorbents such as alkaline aqueous solutions[9] and amines such as ethanolamine,[10] which generally require energy-demanding thermal stripping to release the captured CO_2 for storage and sorbent regeneration (Fig. 1A).[11] Complementary approaches using swings in electrical potential[12,13,14] or applied pressure[15,16] to cycle between capture and release have also been investigated. Regardless of approach, the viability of these mitigation strategies on scale will likely require that their significant energy demand can be ultimately supplied by renewable electricity. As an alternative, we considered whether chemistry can be devised that directly couples CO_2 capture and release to visible light as the only external energy input. Such a system could be *directly* powered by sunlight, for example according to the day-night cycle, and distributed without requiring renewable electricity as an intermediary, along with the costs and limitations associated with its production, storage, distribution, and infrastructure maintenance.

Here, we show that a photoswitchable organic molecule can effectively and repeatedly capture CO_2 from the gas phase and release it on demand upon visible-light exposure. Our study focuses on the well-known spiropyran photochromic dyes,[17,18,19,20] which can be toggled between two forms, a closed spiropyran isomer **SP**, and an open merocyanine isomer **MC**, which differ significantly in chemical properties such as color, acidity, and metal affinity. In particular, dissolved protonated merocyanine (**MCH**$^+$) has been shown to engender large, light-driven pH swings[19] upon irradiation by releasing its proton and cyclizing to **SP**, which is followed by slower thermal reversion to its original state. By coupling this photoinduced equilibrium shift with bicarbonate protonation and carbonic acid dehydration equilibria, we envisioned a system that can sequester CO_2 in the dark but changes its resting state to release that CO_2 upon light exposure. Previous research has demonstrated photoacid-triggered formation of carbonic acid for spectroscopic characterization[21] and photoacid-accelerated CO_2 release from acidic conditions.[22] Very

recently, an elegant strategy using an indazole photoacid to promote CO_2 release from amino acid sorbents was also reported.[23] However, identification of a single-component solute that can recurrently capture and release according to dark/light cycles remains a highly desirable goal. Further, a systematic framework for analyzing the thermodynamic requirements and experimental investigation of the precise mechanism of the photochemical process are needed to provide a theoretical foundation for the development of this novel approach to reversible carbon capture.

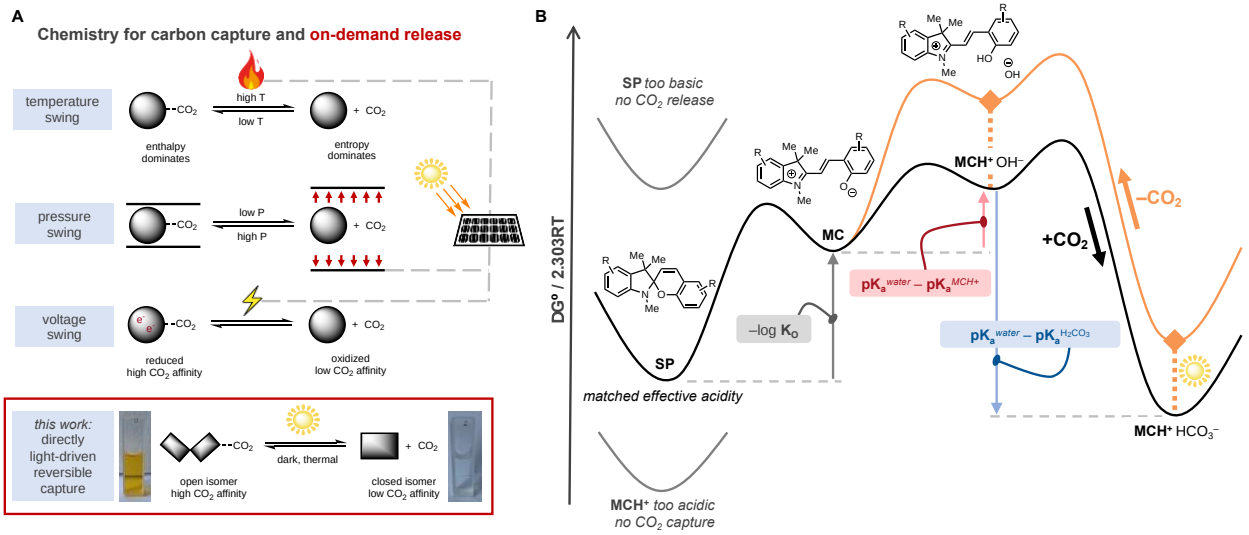

Figure 1. Carbon capture and phototriggered release. (A) Comparison of previously developed chemical processes for reversible CO_2 binding and the new approach in our work. (B) Mechanism for coupling CO_2 capture with photoisomerization of spiropyrans and the required thermodynamic balance. The orange curve shows the rise in average Gibbs free energy of states containing **MCH**$^+$ upon excitation by visible light, reflecting the partial excitation of some members of the ensemble. Compounds for which **MCH**$^+$ is too acidic (**SP** low in energy) will never have **MCH**$^+$ HCO_3^- as the most stable state and therefore will not capture CO_2 effectively. Compounds for which the **SP** form is too basic (**SP** high in energy) will never have **SP** as the most stable state, even with intense irradiation, and therefore will not release CO_2 effectively.

For this proposed process (Fig. 1B), a detailed treatment of the thermodynamic balance shows that precise acidity tuning is critical for the realization of efficient capture and photorelease of CO_2. In solution, a spiropyran **SP** interconverts with an open merocyanine isomer **MC** with an equilibrium constant K_O, typically below unity (favoring **SP**) in aqueous environments[24] (see the SI for additional data regarding solvent effects on the resting state). **MC** features a phenoxide moiety, which can act as a base in aqueous solution and reversibly deprotonate water to form **MCH**$^+$ OH^-. The hydroxide anion can sequester dissolved CO_2 as bicarbonate, and if capture is to be a spontaneous process, we require **MCH**$^+$ HCO_3^- to be the

lowest-energy state in the absence of external energy input. Upon irradiation, some **MCH**$^+$ ions will enter an excited state, the high free energy of which accelerates reversion to **SP** and/or **MC** with release of CO_2 and H_2O. Assuming the kinetically facile pathways exist for interconversion of these various species, the effect of exciting a fraction of **MCH**$^+$ ions is equivalent to elevating the average (ensemble) Gibbs free energy of states containing **MCH**$^+$ by a quantity dependent on the molar absorptivity and integrated photon flux. For effective release of CO_2 to occur, this modification must cause the ensemble free energy of **MCH**$^+$ HCO_3^- and that of **SP** to become inverted relative to their ordering in the dark, such that the latter becomes the lowest-energy state. This cannot be achieved if the relative free energy of **SP** is too high, in which case reversion will require impractically high intensity of light, or if that energy is too low, in which case capture will not occur in the first place. A balanced energetic landscape corresponding to optimal photoswitching of the CO_2 affinity of the solution occurs around (see the SI for a detailed derivation):

$$pK_a(\mathbf{MCH}^+) - \log(1 + K_O^{-1}) \cong pK_a(H_2CO_3).$$

We define the quantity on the left as the apparent conjugate acidity of the spiropyran, pK_{aH}'(**SP**), which accounts for both the Brønsted acidity of the phenol and the driving force for ring closure. The optimal balance of capture and photorelease efficiency should be achieved only by molecules for which pK_{aH}'(**SP**) nears the effective pK_a of H_2CO_3 in its relevant conditions (6.35 in water,[25] although ion-pairing interactions can alter the exact target value, see below).

To validate this analysis, we synthesized spiropyrans **SP1**–**SP8** (Fig. 2), varying in substitution on nitrogen (R^1) and C5 (R^2) of the indoline, as well as on the chromene fragment *ortho* and *para* to the oxygen (R^3). These spiropyran structures can be easily accessed on gram-to-kilogram scale,[26,27,28] usually in a single step from commercial materials. The effective pK_{aH}' values of these molecules in 1:1 DMSO/water were determined by spectrophotometric titration, using the moderate UV absorbance of **SP** and the strong UV-to-visible absorbance of **MCH**$^+$ generated upon isomerization and protonation of **SP**. The parent spiropyran **SP1** is moderately basic (pK_{aH}' = 5.30) in its ground state, and the installation of electron-donating groups on the chromene unit results in the expected increase in basicity of the phenoxide, elevating the pK_{aH}' of **SP3** (R^3 = *o*-OCH_3, pK_{aH}' = 5.51), **SP4** (R^3 = *p*-OCH_3, pK_{aH}' = 5.70), and **SP5** (R^3 = *p*-$N(CH_3)_2$, pK_{aH}' =

5.62) relative to that of **SP1**. Presence of an electron-withdrawing group on the indoline of **SP6** (R^2 = CN), while likely imparting minimal influence on the phenoxide basicity, greatly enhances the effective acidity (pK_{aH}' = 2.91) of the corresponding protonated merocyanine form by favoring the closed, spiropyran form (lowering K_O). The attachment of a solubilizing sulfonate chain on the indoline nitrogen was found to reduce the effective acidity, presumably due to electrostatic effects, as exemplified by **SP7** (R^1 = $(CH_2)_3SO_3^-$, R^3 = *o*-OCH_3, pK_{aH}' = 6.05) and **SP8** (R^1 = $(CH_2)_3SO_3^-$, R^3 = *p*-OCH_3, pK_{aH}' = 6.11).

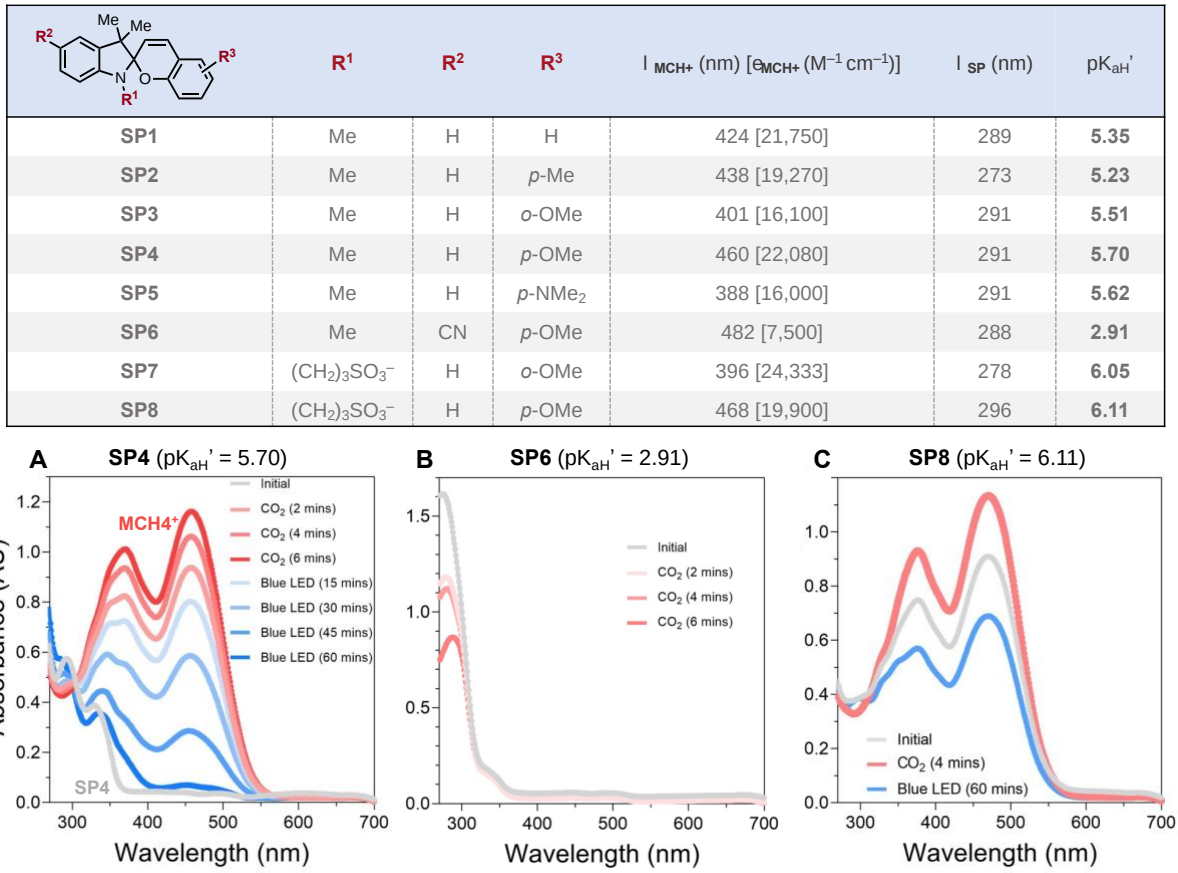

	R^1	R^2	R^3	λ_{MCH+} (nm) [ε_{MCH+} (M^{-1} cm^{-1})]	λ_{SP} (nm)	pK_{aH}'
SP1	Me	H	H	424 [21,750]	289	**5.35**
SP2	Me	H	*p*-Me	438 [19,270]	273	**5.23**
SP3	Me	H	*o*-OMe	401 [16,100]	291	**5.51**
SP4	Me	H	*p*-OMe	460 [22,080]	291	**5.70**
SP5	Me	H	*p*-NMe_2	388 [16,000]	291	**5.62**
SP6	Me	CN	*p*-OMe	482 [7,500]	288	**2.91**
SP7	$(CH_2)_3SO_3^-$	H	*o*-OMe	396 [24,333]	278	**6.05**
SP8	$(CH_2)_3SO_3^-$	H	*p*-OMe	468 [19,900]	296	**6.11**

Figure 2. Spiropyrans: properties and response to CO_2 and light exposure. (top) Summary of spiropyrans evaluated in this work with effective acidities shown on the right. (A) An acidity-matched spiropyran **SP4** captures CO_2 rapidly to generate **MCH4**$^+$ and converts back to its original spiropyran form, releasing CO_2, during irradiation with 450 nm light. (B) A spiropyran **SP6** that is too acidic and therefore does not generate **MCH6**$^+$ in the presence of CO_2. (C) A spiropyran **SP8** that is too basic and already exists in its merocyanine form **MCH8**$^+$ in neutral solution. This material captures CO_2 but does not undergo efficient photorelease.

DMSO–water solutions containing these spiropyrans were evaluated for their competence in the capture of gaseous CO_2 and subsequent release under visible-light irradiation. The range of effective

acidities represented by our panel of candidates allowed us to experimentally confirm our acidity-matching hypothesis, which states that there is an optimal pK_{aH}' for switchable binding to CO_2. In accordance with these predictions, for the most acidic photochromes such as **SP6** (pK_{aH}' = 2.91), exposure to pure CO_2 (1 atm) did not result in any formation of the corresponding protonated merocyanine **MCH6**$^+$ (λ_{max} = 482 nm, Fig. 2B). Conversely, the most basic photochromes such as **SP8** (pK_{aH}' = 6.11), when dissolved in 1:1 DMSO/water, exist significantly in their open isomer **MCH8**$^+$ form (λ_{max} = 468 nm) due to their ability to reversibly deprotonate water (Fig. 2C). Although exposure to pure CO_2 (1 atm) resulted in only a minor increase in the observed quantity of **MCH8**$^+$, a significant amount of CO_2 capture was indicated by the change in pH of the solution from 7.8 to 5.3 (Fig. S9). The weak spectrophotometric response is due to the indistinguishable absorbance profile of **MCH8**$^+$ OH^- and **MCH8**$^+$ HCO_3^-. As anticipated, the latter salt is extremely stable, and irradiation by blue LEDs (λ_{max} = 450 nm) resulted in a relatively small change in the spectrum and 0.7 pH unit increase even after 60 min, reflecting negligible CO_2 release. These negative examples contrast dramatically with the promising results obtained using compounds of moderate acidity such as **SP4** (pK_{aH}' = 5.70) and, to a lesser extent, **SP2** (pK_a' = 5.23). For example (Fig. 2A), exposure of **SP4** to pure CO_2 (1 atm) resulted in rapid and isosbestic conversion to **MCH4**$^+$, which, at this stage, we hypothesized to be paired to HCO_3^-. We proceeded to irradiate this solution with 450 nm blue light, upon which disappearance of **MCH4**$^+$ occurred, accompanied by complete recovery of the original spectrum. Similar but slower conversion in both directions was observed with **SP2**. This compound is also significantly less soluble than **SP4** (26 mM *vs.* < 3 mM for **SP2**), so we elected to proceed with **SP4** for the ensuing analysis (see the SI for evaluation of other dyes and extended discussion regarding the selection of **SP4**).

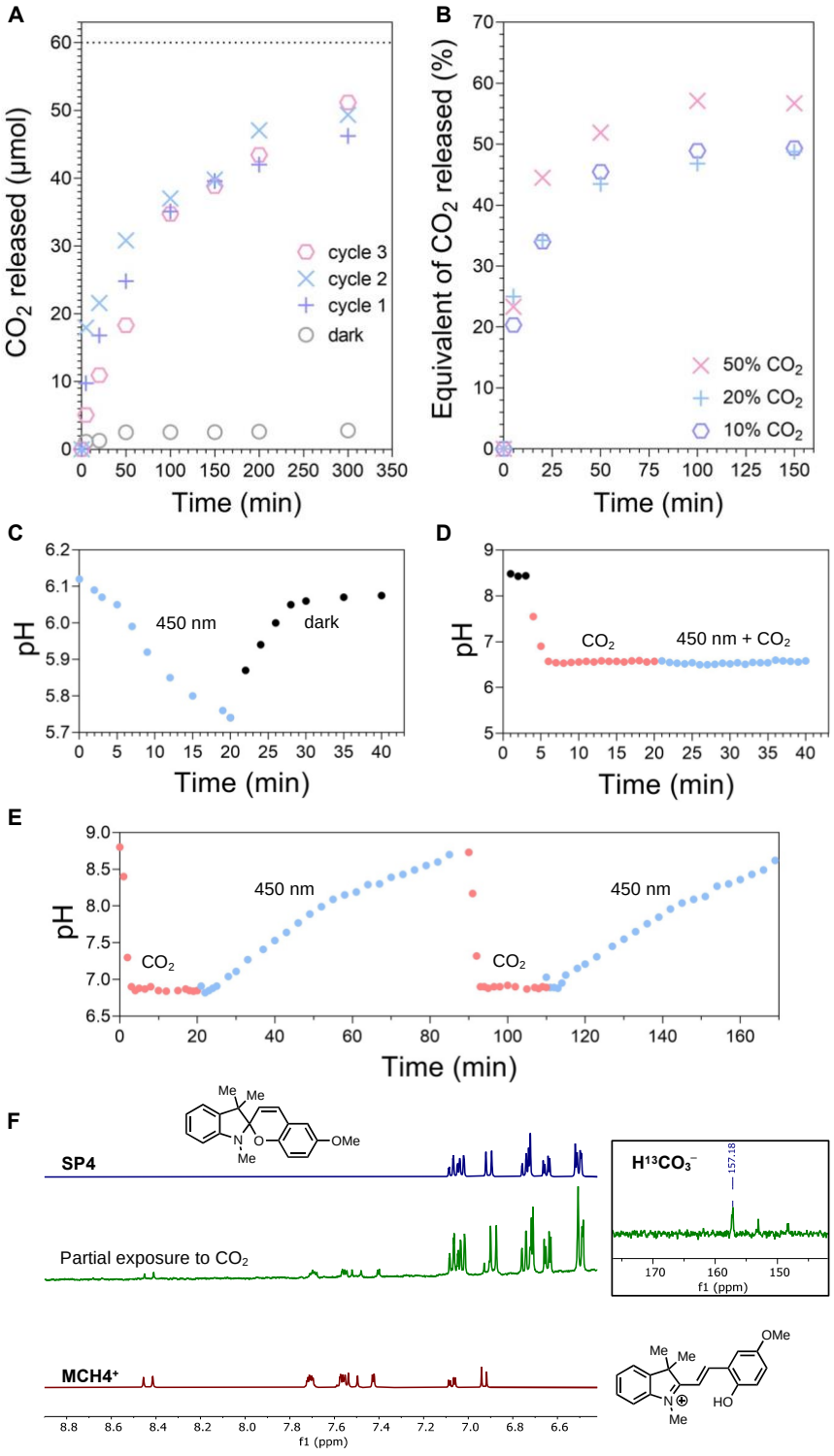

Figure 3. CO_2 passive capture and photorelease: performance and mechanism. (A) GC quantification of released CO_2 from three consecutive cycles of exposure to CO_2 and blue light (450 nm) irradiation, including a control replicate performed with the sample wrapped in reflective foil. (B) Released CO_2 after capture from CO_2/N_2 mixtures. (C,D,E) *In situ* pH tracking of a DMSO–water solution of **SP4** under different conditions. (F) NMR spectroscopic evidence for **MCH4**$^+$ $HCO3^-$ as the resting state of the captured CO_2.

Successful repeated capture and light-triggered release of CO_2 by **SP4** was confirmed by quantitative gas chromatography (GC) calibrated against standard mixtures (Fig. 3A). After introduction of CO_2 into a solution of **SP4** (60 μmol in 3 mL solvent, 4:1 DMSO/water), which effected the appearance of an intense yellow color, the vial headspace was replaced with nitrogen and the cuvette was exposed to 450 nm light. Aliquots of the gas in the headspace were analyzed, and the gaseous CO_2 content was observed to increase over time (half-life of *ca.* 60 min) to a terminal value of 46–51 μmol, representing on average 81% of theoretical capture capacity. The now-colorless solution was then immediately re-exposed to CO_2, and photorelease procedure performed again for a total of three capture–release cycles. No difference in activity was observed, implying that the spiropyran dye shows stability under these operating conditions, including extended exposure to atmospheric oxygen, which is not tolerated by most molecular redox approaches. Temperature control during irradiation was carefully maintained using portable fans, and control experiments in which the sample was shielded from light by reflective foil displayed negligible release of CO_2. Spectrophotometry further confirmed that release in the dark is extremely slow even when opened to the atmosphere (11.5% decrease in **MCH4**$^+$ HCO_3^- over 9 h, see SI for details). Pure gas input was not required for capture (Fig. 3B): using 50%, 20%, and 10% v/v mixtures of CO_2 in N_2 delivered similar results, although the total quantity of CO_2 released relative to **SP4** decreased to roughly 50% in the most dilute case. Nevertheless, these experiments prove the concept of cyclic carbon capture and release using visible light as the only external energy input.

To further illustrate key mechanistic aspects of the capture and release processes, *in situ* pH tracking experiments were conducted (Fig. 3C–E), which revealed a shift between pH-determining species resulting from the coupling of multiple equilibria. First, hydrochloric acid was added to partially convert **SP4** to the **MCH4**$^+$ Cl^- form. The protonated cation is a metastable-state photoacid that, upon irradiation, converts to **SP4** while releasing a proton to solvent, and accordingly, a decrease in the measured pH was measured. Upon removal of the light source, the pH rapidly recovered to its starting value as **SP4** thermally reverts to **MC4**, which is rapidly reprotonated. If instead of using a strong acid, equilibration with an atmosphere of

CO_2 was used to open **SP4** to its protonated merocyanine form, identical irradiation conditions resulted in no noticeable change in pH provided the solution remained in equilibrium with an applied pressure of CO_2. This difference is due to buffering capacity of bicarbonate, as the photoreaction of **MCH4**$^+$ now prompts net proton transfer to bicarbonate rather than the solvent, and therefore cannot be perceived by pH measurement. Under a headspace of pure CO_2, the carbonic acid remains in solution and can return the proton to **SP4**. If the CO_2-charged solution is opened to the air such that carbonic acid can favorably dehydrate to form CO_2 and escape into the headspace, photoirradiation results in a steady *increase* in the solution pH. The photoacidic activity of **MCH4**$^+$ results in a net *basification* of the solution because the released proton is not received by solvent but participates with bicarbonate in an irreversible process ($H_2CO_{3(aq)} \rightarrow H_2O_{(l)} + CO_{2(g)}$) that depletes carbonic acid, which was the prevailing acidic species. The pH could then revert to its starting point with removal of the light source and equilibration with an atmosphere of CO_2.

The assignment of dominant dissolved inorganic carbon species as **MCH4**$^+$ HCO_3^-, as opposed to a direct covalent adduct such as **MC4-CO$_2$** could not be established on the basis of spectrophotometry alone, as TD-DFT calculations indicate that the lowest-energy excitations are similar in energy for free **MCH4**$^+$ (497 nm), **MCH4**$^+\cdots HCO_3^-$ (509 nm), and **MC4-CO$_2$** (473 nm), and all are close to the experimental λ_{max} (460 nm). However, the identity of the cation as **MCH4**$^+$ is apparent from ^{1}H NMR spectroscopy (Fig. 3F): the protonated merocyanine could be independently prepared by protonation of **SP4** with strong acid, and partial exposure of **SP4** to gaseous CO_2 resulted in evolution of identical resonances in the ^{1}H NMR. When this same spiropyran was exposed to ^{13}C-labelled CO_2, a broad resonance arose in the ^{13}C NMR spectrum at 157.2 ppm, which matches the chemical shift of the [^{13}C]-bicarbonate anion.

Having established the relevant ground-state structures involved in the light-driven capture cycle, we turned to further dissecting the mechanism of the photorelease subprocess. Three plausible pathways were considered (Fig. 4A): (A) a non-photoacid mechanism, involving reversible formation of adduct **MC4-CO$_2$** and subsequent photoinduced cleavage of the O–CO_2^- bond; (B) a specific photoacid

mechanism, in which **MCH4**$^+$ releases its proton to water upon irradiation, and the solvent serves to transfer this proton to a separated or distant HCO_3^- to form carbonic acid; and (C) a general photoacid mechanism, in which **MCH4**$^+$ and HCO_3^- as a contact ion pair directly exchange a proton in the excited state.

A solution containing **MCH4**$^+$ HCO_3^- was prepared by bubbling CO_2 into dissolved **SP4**, and the excited-state dynamics of this species were investigated by ultrafast transient absorption spectroscopy (Fig. 4B). After excitation using a 400 nm laser pulse, significant excited-state absorption (ESA) was observed at 530 nm. We assigned this feature to **MC4*** obtained upon deprotonation of **MCH4**$^{+}$* in its excited state. The decay of ESA intensity at 530 nm fit well with a biexponential function with time constants τ_1 = 7 ps and τ_2 = 52 ps (Fig. 4C). As examined further below, we propose these first-order decays are respectively associated with proton-transfer (PT) and reverse-proton-transfer (rev-PT) processes from **MCH4**$^+$ to water.

A significant kinetic isotope effect (KIE) was observed in the rates of both steps by using D_2O as an alternative solvent (τ_1 = 7 ps using H_2O *vs.* τ_1 = 11 ps using D_2O, KIE = 1.6; τ_2 = 52 ps using H_2O *vs.* τ_2 = 80 ps using D_2O, KIE = 1.5, Fig. 4D). The magnitudes of these deuterium isotope effects are potentially consistent with proton transfer between two heteroatomic sites of widely differing acidities (mechanisms B and C). These results would be more difficult to rationalize in a non-photoacid pathway such as mechanism A, in which no primary isotope effect should manifest. The same transient absorption experiments were also repeated with **MCH4**$^+$ Cl^- and **MCD4**$^+$ Cl^-, and time constants (τ_1 = 5 ps using HCl *vs.* τ_1 = 12 ps using DCl, KIE = 2.4; τ_2 = 46 ps using HCl *vs.* τ_2 = 73 ps using DCl, KIE = 1.6) were found to be similar to those measured with bicarbonate, suggesting that the initial acceptor of the merocyanine-derived proton was not the anion. This observation led us to favor mechanism B, in which the immediate target is a solvent (water) molecule.

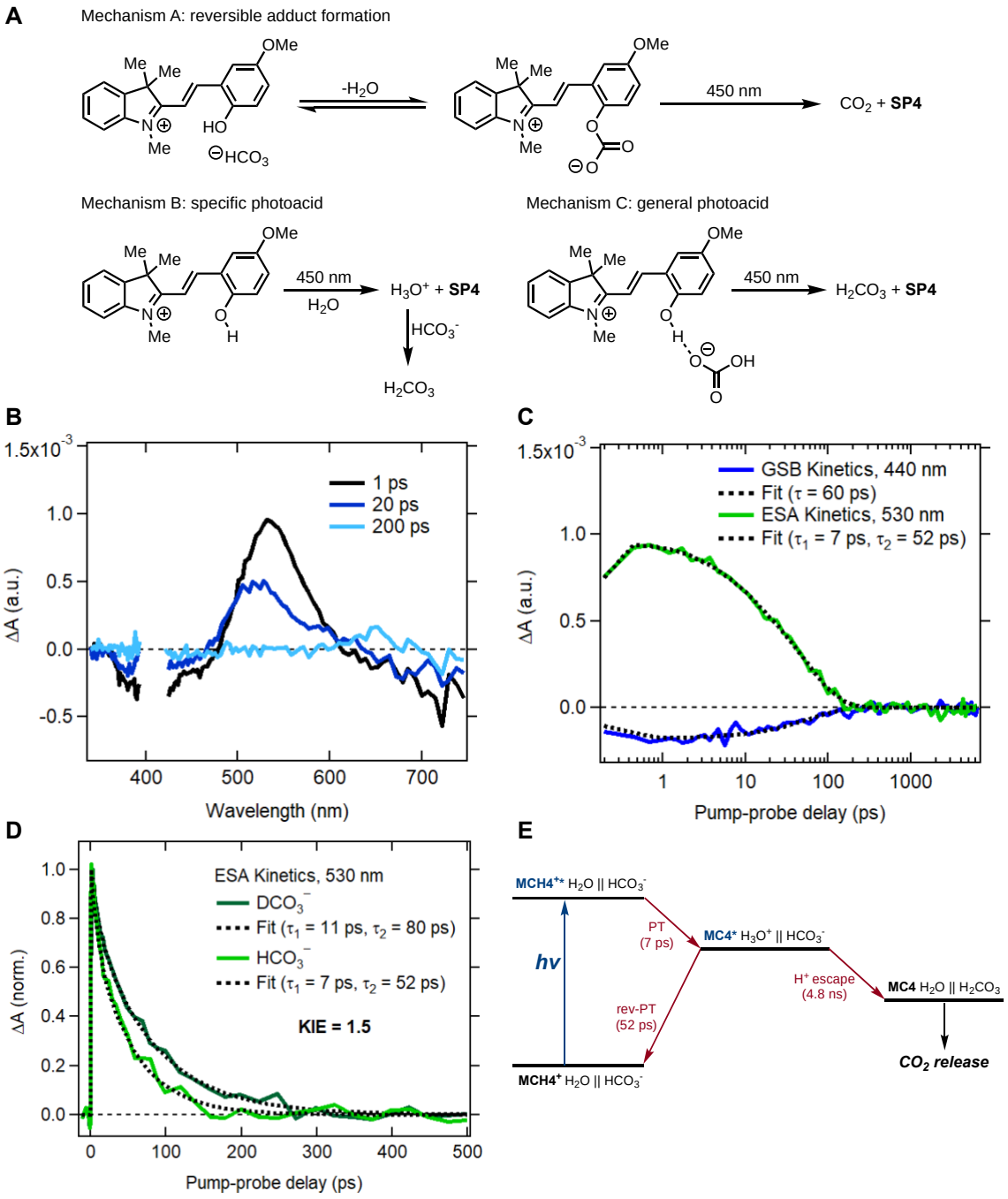

Figure 4. Mechanism of CO_2 photorelease. (A) Three mechanistic proposals considered in this study. (B) Transient absorption spectra of **MCH4**$^+$ HCO_3^-, with excitation at 400 nm. Laser scattering region was removed for clarity. (C) Decay kinetics of the ground-state bleach (GSB) and excited-state absorption (ESA) features with exponential and biexponential fits, respectively. (D) Comparative decay profiles of the ESA using **MCH4**$^+$ HCO_3^- and **MCD4**$^+$ DCO_3^-, showing a kinetic isotope effect of ~1.5 for both processes represented in the biexponential kinetic model. (E) Proposed scheme for CO_2 release after initial electronic excitation of **MCH4**$^+$. Ions divided by double vertical lines indicate a solvent-separated ion pair, in which the ions are not directly in contact, but separated by few enough solvent molecules that the anion still exerts a detectable influence on the reactivity of the cation.

Fig. 4E summarizes the proposed overall scheme for light-driven generation of carbonic acid from the **MCH4**$^+$ HCO_3^-. After photoexcitation of **MCH4**$^+$, rapid proton transfer (τ = 7 ps) takes place from the merocyanine to a hydrogen-bonded water molecule with minimal heavy-atom motion, forming a hydrogen-bonded excited state complex [**MC4***$\cdots H_3O^+$]. This complex can either undergo reverse proton transfer (τ = 52 ps) to restore the initial **MCH4**$^+$, or the proton can diffuse away through a von Grotthuss–type mechanism[29,30,31] to find a basic bicarbonate anion. Based on a quantum yield of 1.3% for the formation of **MC4** derived from nanosecond transient absorption spectroscopy, the proton escape takes place on the order of *ca.* 4.8 ns.

Interestingly, when the sample was prepared such that the anion was instead a chloride, we found a minor but verifiable decrease in the quantum yield (1.1%), indicating likely involvement of the counteranion in regulating competition between the reverse-proton-transfer and proton-escape pathways. Thus, the nature of **MCH4**$^+$ HCO_3^- under these conditions is most aptly described as a solvent-separated ion pair,[32,33] rather than as free ions. The electrostatically associated bicarbonate is not the direct recipient of the proton from **MCH4**$^+$ but does remain sufficiently proximal to influence the preorganization of the intervening solvent molecule(s) and thereby the frequency of carbonic acid formation. If accurate, this scheme is informative for optimizing the rate of CO_2 photogeneration. For example, structural modifications that promote dissociation of hydronium from the **MC4**$\cdots H_3O^+$ complex might reduce the rate of reverse proton transfer, while strengthening of the attractive interactions between **MCH4**$^+$ and HCO_3^- should accelerate the productive protonation of bicarbonate. Studies into implementing these design principles and other modifications aimed at maximizing solubility, synthetic scalability, longevity, and wavelength coverage are ongoing, with the long-term intention of generalizing solar-powered carbon removal technologies.

Acknowledgements

A.M.A acknowledges King Faud University of Petroleum and Minerals and the Ministry of Education of Saudi Arabia for a doctoral scholarship. A.M.A., T.Y.G., and M.J.A. thank the Harvard Climate Change Solutions Fund for partial support. The authors are grateful to Prof. George M. Whitesides (Harvard) for the use of gas chromatography (GC) and other instrumentation and for insightful comments.

References

[1] Minx, J. C.; Lamb, W. F.; Callaghan, M. W.; Fuss, S.; Hilaire, J.; Creutzig, F.; Amann, T.; Beringer, T.; Garcia, W. d. O.; Hartmann, J. Negative Emissions—Part 1: Research Landscape and Synthesis. *Environ. Res. Lett.* **2018**, *13* (6), 063001. DOI: 10.1088/1748-9326/aabf9b.

[2] Intergovernmental Panel on Climate Change. Climate Change 2021: The Physical Science Basis: Contribution of Working Group I to the Sixth Assessment Report of the Intergovernmental Panel of Climate Change. Cambridge University Press: Cambridge, UK, 2021.

[3] Intergovernmental Panel on Climate Change. Climate Change 2014: Mitigation of Climate Change: Working Group III Contribution to the IPCC Fifth Assessment Report. Cambridge University Press: Cambridge, UK, 2014. DOI:10.1017/CBO9781107415416.

[4] Giorgi, F.; Whetton, P. H.; Jones, R. G.; Christensen, J. H.; Mearns, L. O.; Hewitson, B.; vonStorch, H.; Francisco, R.; Jack, C. Emerging Patterns of Simulated Regional Climatic Changes for the 21st Century Due to Anthropogenic Forcings. *Geophys. Res. Lett.* **2001**, *28* (17), 3317–3320. DOI:10.1029/2001gl013150.

[5] Leung, D. Y. C.; Caramanna, G.; Maroto-Valer, M. M. An Overview of Current Status of Carbon Dioxide Capture and Storage Technologies. *Renew. Sustain. Energy Rev.* **2014**, *39*, 426– 443. DOI: 10.1016/j.rser.2014.07.093.

[6] Gibbins, J.; Chalmers, H. Carbon Capture and Storage. *Energy Policy* **2008**, *36* (12), 4317–4322. DOI: 10.1016/j.enpol.2008.09.058.

[7] Hanna, R.; Abdulla, A.; Xu, Y.; Victor, D. G. Emergency Deployment of Direct Air Capture as a Response to the Climate Crisis. *Nat. Commun.* **2021**, *12*, 368. DOI: 10.1038/s41467-020-20437-0.

[8] Sanz-Pérez, E. S.; Murdock, C. R.; Didas, S. A.; Jones, C. W. Direct Capture of CO_2 from Ambient Air. *Chem. Rev.* **2016**, *116* (19), 11840–11876. DOI: 10.1021/acs.chemrev.6b00173.

[9] Keith, D. W.; Holmes, G.; St. Angelo, D.; Heidel, K. A Process fo Capturing CO_2 from the Atmosphere. *Joule* **2008**, *2* (8), 1573–1594. DOI: 10.1016/j.joule.2018.05.006.

[10] Rochelle, G. T. Amine Scrubbing for CO_2 Capture. *Science* **2009**, *325* (5948), 1652–1654. DOI: 10.1126/science.1176731.

[11] Mazari, S. A.; Si Ali, B.; Jan, B. M.; Saeed, I. M.; Nizamuddin, S. An Overview of Solvent Management and Emissions of Amine-Based CO_2 Capture Technology. *Int. J. Greenh. Gas Control* **2015**, *34*, 129–140. DOI: 10.1016/j.ijggc.2014.12.017.

[12] Jin, S.; Wu, M.; Gordon, R. G.; Aziz, M. J.; Kwabi, D. G. pH Swing Cycle for CO_2 Capture Electrochemically Driven Through Proton-Coupled Electron Transfer. *Energy Environ. Sci.* **2020**, *13*, 3706–3722. DOI: 10.1039/D0EE01834A.

[13] Voskian, S.; Hatton, T. A. Faradaic Electro-Swing Reactive Adsorption for CO_2 Capture. *Energy Environ. Sci.* **2019**, *12*, 3530–3547. DOI: 10.1039/C9EE02412C.

[14] Sharifian, R.; Wagterveld, R. M.; Digdaya, I. A.; Xiang, C.; Vermaas, D. A. Electrochemical Carbon Dioxide Capture to Close the Carbon Cycle. *Energy Environ. Sci.* **2021**, *14*, 781–814. DOI: 10.1039/D0EE03382K.

[15] Ho, M. T.; Allinson, G. W.; Wiley, D. E. Reducing the Cost of CO_2 Capture from Flue Gases Using Pressure Swing Adsorption. *Ind. Eng. Chem. Res.* **2008**, *47* (14), 4883–4890. DOI: 10.1021/ie070831e.

[16] Siqueira, R. M.; Freitas, G. R.; Peixoto, H. R.; do Nascimento, J. F.; Musse, A. P. S.; Torres, A. E. B.; Azevedo, D. C. S.; Bastos-Neto, M. Carbon Dioxide Capture by Pressure Swing Adsorption. *Energy Procedia* **2017**, *114*, 2182–2192. DOI: 10.1016/j.egypro.2017.03.1355.

[17] Kortekaas, L.; Browned, W. R. The Evolution of Spiropyran: Fundamentals and Progress of an Extraordinarily Versatile Photochrome. *Chem. Soc. Rev.* **2019**, *48*, 3406–3424. DOI: 10.1039/C9CS00203K.

[18] Klajn, R. Spiropyran-Based Dynamic Materials. *Chem. Soc. Rev.* **2013**, *43*, 148–184. DOI: 10.1039/C3CS60181A.

[19] Wimberger, L.; Prasad, S. K. K.; Peeks, M. D.; Andréasson, J.; Schmidt, T. W.; Beves, J. E. Large, Tunable, and Reversible pH Changes by Merocyanine Photoacids. *J. Am. Chem. Soc.* **2021**, *143* (49), 20758–20768. DOI: 10.1021/jacs.1c08810.

[20] Liao, Y. Design and Applications of Metastable-State Photoacids. *Acc. Chem. Res.* **2017**, *50* (8), 1956–1964. DOI: 10.1021/acs.accounts.7b00190.

[21] Adamczyk, K.; Prémont-Schwarz, M.; Pines, D.; Pines, E.; Nibbering, E. T. J. *Science* **2009**, *326* (5960), 1690–1694. DOI: 10.1126/science.1180060.

[22] Bennett, R.; Clifford, S.; Anderson, K.; Puxty, G. Carbon Capture Powered by Solar Energy. *Energy Procedia* **2017**, *114*, 1–6. DOI: 10.1016/j.egypro.2017.03.1139.

[23] Premadasa, U. I.; Bocharova, V.; Miles, A. R.; Stamberga, D.; Belony, S.; Bryantsev, V. S.; Elgattar, A.; Liao, Y.; Damron, M. K.; Doughty, B.; Custelcean, R.; Ma, Y. Photochemically-Driven CO_2 Release Using a Metastable-State Photoacid for Energy Efficient Direct Air Capture. *Angew. Chem. Int. Ed.* **2023**, *in press.* DOI: 10.1002/anie.202304957.

[24] Berton, C.; Pezzato, C. Photoacidity of Indolinospirobenzopyrans in Water. *Eur. J. Org. Chem.* **2023**, *26* (17), e202300070. DOI: 10.1002/ejoc.202300070.

[25] Zeebe, R. E.; Wolf-Gladrow, D. CO_2 in Seawater: Equilibrium, Kinetics, Isotopes, Elsevier Oceanography Series 65. Elsevier: Amsterdam, Netherlands, 2001.

[26] Barbee, M. H.; Mondal, K.; Deng, J. Z.; Bharambe, V.; Neumann, T. V.; Adams, J. J.; Boechler, N.; Dickey, M. D.; Craig, S. L. Mechanochromic Stretchable Electronics. *ACS Appl. Mater. Interfaces* **2018**, *10* (35), 29918–29924. DOI: 10.1021/acsami.8b09130.

[27] Yang, H.; Hu, W.; Sun, C.; Ren, Y.; Qin, S.; Huang, J. Spiropyrane Derivative with Color, Fluorescence and Liquid Crystal Property Triple Switching Effects as Well as Preparation Method and Application Thereof. China Patent CN113024571, June 25, 2021.

[28] Wang, M.; Zhang, H.; Ji, L.; Fan, W.; Qiao, Z.; Si, Y.; Wang, Z.; Zheng, Y.; Xue, X.; Wu, X.; Liu, Y. Photochromic Optical Material. China Patent CN107722028, February 23, 2018.

[29] Mohammed, O. F.; Pines, D.; Dreyer, J.; Pines, E.; Nibbering, E. T. J. Sequential Proton Transfer Through Water Bridges in Acid-Base Reactions. *Science* **2005**, *310* (5745), 83–86. DOI: 10.1126/science.1117756.

[30] Rini, M.; Magnes, B.-Z.; Pines, E.; Nibbering, E. T. J. Real-Time Observation of Bimodal Proton Transfer in Acid-Base Pairs in Water. *Science* **2003**, *301* (5631), 349–352. DOI: 10.1126/science.1085762.

[31] Mohammed, O. F.; Pines, D.; Nibbering, E. T. J.; Pines, E. Base-Induced Solvent Switches in Acid-Base Reactions. *Angew. Chem. Int. Ed.* **2007**, *46* (9), 1458–1461. DOI: 10.1002/anie.200603383.

[32] Winstein, S.; Clippinger, E.; Fainberg, A. H.; Heck, R.; Robinson, G. C. Salt Effects and Ion Pairs in Solvolysis and Related Reactions. III. Common Ion Rate Depression and Exchange of Anions during Acetolysis. *J. Am. Chem. Soc.* **1956**, *78* (2), 328–335. DOI: 10.1021/ja01583a022.

[33] Bentley, T. W.; Schleyer, P. von R. Medium Effects on the Rates and Mechanisms of Solvolytic Reactions. *Adv. Phys. Org. Chem.* **1977**, *14*, 1–67. DOI: 10.1016/S0065-3160(08)60107-0.